Physics Letters A 375 (2011) 633–637

Contents lists available at ScienceDirect

Physics Letters A

www.elsevier.com/locate/pla

Stability of $BiAlO_3$ and its vacancy defects: A first-principles study

Zhiping Lin [a,b,*], Yu-Jun Zhao [a], Yanming Zhao [a]

[a] Department of Physics, South China University of Technology, Guangzhou 510640, China
[b] School of Physics, Guangdong University of Technology, Guangzhou 510090, China

ARTICLE INFO

Article history:
Received 28 September 2010
Received in revised form 30 October 2010
Accepted 2 November 2010
Available online 5 November 2010
Communicated by R. Wu

Keywords:
Ferroelectricity
First-principles
Formation energy
Charged vacancy

ABSTRACT

Through first-principles calculations and thermodynamic analysis, we investigate the stable chemical potential range for $BiAlO_3$ with *R3c* and *Pm3m* symmetry. The possible vacancies of $BiAlO_3$ are mostly at their charged state rather than neutral state. And vacancies are more easily formed in *R3c* system than *Pm3m* system under same condition.

1. Introduction

Bi-based compounds have received particular interests as lead-free materials for ferroelectric thin film materials and devices [1,2]. They are nontoxic and also have $6s^2$ lone pair electrons that cause large structural distortions from the prototypical cubic perovskite phase and in turn strong coupling between the electronic and structural degrees of freedom [3,4]. Recently, Baettig et al. [5] theoretically predicted a large ferroelectric polarization and piezoelectricity in the hypothetical perovskite-structure oxides bismuth aluminate ($BiAlO_3$) and bismuth galliate ($BiGaO_3$). $BiAlO_3$ was predicted to have a noncentrosymmetric and polar *R3c* symmetry as shown in Fig. 1(a), good piezoelectric properties and a high ferroelectric T_c of $\sim 530\,^{\circ}C$. The dielectric properties of $BiAlO_3$ reflects that there are some irreversible changes occurring around $200\,^{\circ}C$ during the synthesis [6]. It is suggested that there are charged (positive and negative) defects presented in the sample after synthesis, and these relatively slow-moving defects may result in a decrease of the magnitude of the dielectric anomaly with increasing frequency. A similar dielectric effect has been observed in $Ba_{1-x}Pb_xTiO_3$ ceramics [7], whose anomaly dielectric was attributed to the movement of charged defects and could disappear by changing the synthetic conditions.

Vacancies are one of the fundamental and intrinsic defects in perovskite oxides and give a critical impact on their properties such as the remnant polarization, motion of domain walls, dielectric constant and leakage current. A Pb vacancy in $PbTiO_3$, when forming a Pb–O vacancy pair with a compensated oxygen vacancy, possesses a dipole moment twice as large as a Pb vacancy in the bulk $PbTiO_3$ [8]. Oxygen vacancies play an essential role in polarization degradation phenomena such as fatigue and aging [9,10], and may also be responsible for imprint (i.e., history-dependent up–down asymmetry) phenomena with the coexistence of impurities. The oxygen vacancy defect has a tendency to be pinned at the domain boundary when it is formed near a domain wall [11] and is often created intentionally to obtain a high conductivity. For instance, oxygen vacancies in $SrTiO_3$ were shown to generate carrier mobility as high as $10^4\ cm^2\,V^{-1}\,s^{-1}$ at low temperature [12]. The key to take advantage of the defects is to control the concentration

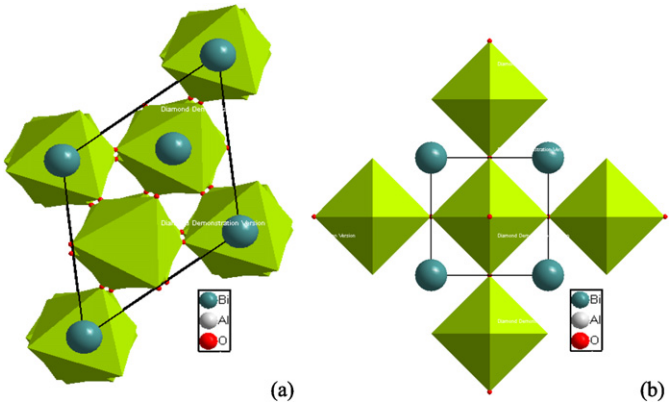

Fig. 1. The crystal structure of $BiAlO_3$ (a) with a space group *R3c* (b) with space group *Pm3m*.

* Corresponding author at: Department of Physics, South China University of Technology, Guangzhou 510640, China.
E-mail address: zhp_lin@sohu.com (Z. Lin).

0375-9601/$ – see front matter
doi:10.1016/j.physleta.2010.11.013

Table 1
The relaxed lattice parameters and the Wyckoff positions of atoms in $BiAlO_3$ compared with experimental data [2].

Site	Wyckoff position	Calculated	Experimental
Bi	6a	(0.0000, 0.0000, 0.0061)	(0.0000, 0.0000, 0.0000)
Al	6a	(0.0000, 0.0000, 0.2213)	(0.0000, 0.0000, 0.2222)
O	18b	(0.5505, 0.0100, 0.9604)	(0.5326, 0.0099, 0.9581)
a (Å)		5.3981	5.3754
c (Å)		13.376	13.393

of defects technically, which is basically tuned by the temperature and chemical environment of the sample sintering condition, and reflected theoretically by their formation energies and corresponding thermodynamic equilibrium. The formation energy of a vacancy is defined as the energy required removing an atom from the host material and placing it into a corresponding reservoir of the same chemical potential. In this Letter, we focus on the oxygen and metal vacancies in $BiAlO_3$, which remarkably depends on the synthetic conditions. We hope that the quantitative calculation of these vacancy formation energies will be beneficial to the understanding of the ferroelectrics in $BiAlO_3$.

2. Theoretical methods

A critical factor affecting the vacancy formation energy is the chemical environment of the sintering condition, which is described by atomic chemical potentials [13]. Under equilibrium, the chemical potential of an atom is defined as the Gibbs free energy of the atom in equilibrium with the system. The energy of an atom in its elemental solid is often taken as a reference for its chemical potential [13,14]. Although the chemical potentials are affected by the ambient pressure and/or temperature, they are constrained by thermodynamic equilibrium conditions and the requirement of avoiding unwanted secondary phases. The valid range of chemical potentials is required for one to tune the concentration of corresponding defects.

Firstly, the atomic potential should be lower than that of their corresponding elemental solid to avoid precipitation of solid elemental crystal, which gives

$$\Delta\mu_{\mathrm{Al}} \leqslant 0, \qquad \Delta\mu_{\mathrm{Bi}} \leqslant 0, \quad \text{and} \quad \Delta\mu_{\mathrm{O}} \leqslant 0 \tag{1}$$

$\Delta\mu = \mu - \mu^{solid}$, which is the chemical potential relative to that of corresponding element solid. Secondly, in the state of equilibrium, the sum of chemical potentials for all atoms equals to the heat of formation to maintain a stable compound. That is

$$\Delta\mu_{\mathrm{Al}} + \Delta\mu_{\mathrm{Bi}} + 3\Delta\mu_{\mathrm{O}} = \Delta H(\mathrm{BiAlO_3}). \tag{2}$$

Here $\Delta H(\mathrm{BiAlO_3})$ is the formation enthalpy of $BiAlO_3$. In addition, the chemical potentials are further restricted with their possible competing phases formed with Al, Bi, and O atoms.

$$2\mu_{\mathrm{Al}} + 3\mu_{\mathrm{O}} \leqslant \Delta H(\mathrm{Al_2O_3}), \qquad 2\mu_{\mathrm{Bi}} + 3\mu_{\mathrm{O}} \leqslant \Delta H(\mathrm{Bi_2O_3}). \tag{3}$$

With the calculated formation enthalpies, valid ranges of chemical potential μ_{Al}, μ_{Bi}, and μ_{O} can be determined by Eqs. (1)–(3).

The formation enthalpy of vacancy with a charge state q is determined according to [13]

$$\Delta H^{(V_i,q)} = E(V_i,q) - E(0) + \left(\Delta\mu_i + \mu_i^{element}\right) + q(E_{VBM} + E_F), \tag{4}$$

where $E(V_i,q)$ and $E(0)$ are the total energies of the supercell with and without a vacancy V_i. $\Delta\mu_i + \mu_i^{element}$ is the chemical potential of atom i at the sintering condition. E_{VBM} represents the energy at the valence band maximum of the defect free system, while E_F is the Fermi energy relative to the E_{VBM}.

Detailed first-principles density functional calculations are performed using Vienna Ab initio Simulation Package (VASP) [15]. We used the GGA approximation of PW91 formulism [16], while the electron–ion interactions were described by the PAW pseudopotentials [17]. The $BiAlO_3$ compound considered here has an isotopic structure with multiferroic perovskite-like $BiFeO_3$ with space group $R3c$ [2], whose computed Wyckoff atom positions are listed in Table 1, which are clearly in good agreement with the experimental values. The valence configurations include the O $2s$ and $2p$, the Al $3s$, $3p$, and $4s$, and the Bi $5d$, $6s$, and $6p$ electrons in the calculations. We employ a $3 \times 1 \times 1$ supercell of 90 atoms to calculate the formation energy of vacancy defects. The wave functions were expanded in plane waves with an energy cutoff of 500 eV. Brillouin zone integration of band structure was performed with a $5 \times 5 \times 2$ Monkhorst–Pack mesh for the single cell and $3 \times 3 \times 2$ Monkhorst–Pack mesh for the $3 \times 1 \times 1$ supercell. The total energies for the structures were converged within 10^{-3} eV with respect to k-points. Fermi level is smeared by the Gaussian method with a width of 0.1 eV during the self-consistent calculation.

3. Results and discussions

3.1. Allowed chemical potential range for $BiAlO_3$

In order to obtain the valid range of chemical potential, we firstly calculated the formation enthalpies of bulk $BiAlO_3$, bulk Bi, Al as well as oxygen-related compounds. Table 2 lists the calculated lattice constants of perfect bulk cells of elemental solids (Bi and Al) and compound solids (Al_2O_3, Bi_2O_3 and $BiAlO_3$). The $BiAlO_3$ with space group $Pm3m$ (the crystal structure is shown in Fig. 1(b)) is considered. It can be seen that theoretical results is in good agreement with the experimental data and is consistent with theoretical results (5.29 Å and 13.24 Å for hexagonal-$BiAlO_3$ [18] and 3.724 Å for $Pm3m$ structure [19]) calculated by Wien2k code. For oxygen molecules, the total energy obtained -4.396 eV/O by non-spin-polarized calculation and -4.89 eV/O [20] by spin-polarized calculation are lower than the experimental result, and then the experimental value is adopted in the calculation.

The formation enthalpy ΔH of compound $BiAlO_3$ per molecular formula is given by $\Delta H(\mathrm{BiAlO_3}) = E_{total}(\mathrm{BiAlO_3}) - E_{total}(\mathrm{Bi}) - E_{total}(\mathrm{Al}) - \frac{3}{2}E_{total}(\mathrm{O_2})$, where E_{total} is the density-functional total energy of each component. The formation enthalpies of Al_2O_3 and Bi_2O_3 compounds are calculated according to the chemical reactions $2\mathrm{Al} + 3/2\mathrm{O_2} = \mathrm{Al_2O_3}$ and $2\mathrm{Bi} + 3/2\mathrm{O_2} = \mathrm{Bi_2O_3}$, respectively. The calculated formation enthalpies are given in Table 2. It can be seen that the theoretical formation enthalpy of -17.22 eV for Al_2O_3 is in accordance with the experimental value (-16.75 eV) [19]. For Bi_2O_3, the discrepancy between theory and experiment is rather small (~ 0.011 eV). The compound for $BiAlO_3$ can be obtained by the stoichiometric mixture of Al_2O_3 and Bi_2O_3. Therefore, $\Delta H(\mathrm{BiAlO_3})$ should be lower than corresponding formation energy in Al_2O_3 or Bi_2O_3, i.e. < -11.245 eV. In addition, it indicates that the formation energies satisfy the relation of $\frac{1}{2}|\Delta H(\mathrm{Bi_2O_3})| \leqslant \frac{1}{2}|\Delta H(\mathrm{Al_2O_3})| \leqslant |\Delta H(\mathrm{BiAlO_3})|$ (cf. Table 2), which is in analogy with that of barium titanate and lead titanate compounds as discussed in Ref. [21].

The allowed chemical potential range of $BiAlO_3$ is required to satisfy Eqs. (1)–(3) to maintain the equilibrium of $BiAlO_3$ solid without any secondary phases. The chemical potential of bismuth,

Table 2
Calculated lattice parameters (a and/or c) of bulk solids and formation enthalpies of compounds per chemical formula, obtained from the present calculations. Available experimental results from Ref. [20] are listed in the bracket for comparison.

Materials	a (Å)	b (Å)	c (Å)	ΔH (eV)	
				Theoretical	Experimental*
Bi (bcc)	8.496 (8.518)			−2.19	−2.15
Al (fcc)	3.965 (4.049)			−3.64	−3.34
Al_2O_3 (R-3cH)*	4.723 (4.759)		12.904 (12.993)	−17.22	−16.76
Bi_2O_3 (P121/C1)*	5.8443	8.1040	7.2827	−5.73	−5.74
	(5.8444)	(8.1574)	(7.4032)		
$BiAlO_3$ (*R3c*)	5.398 (5.375)		13.375 (13.393)	−12.617	
$BiAlO_3$ (*Pm3m*)	3.783 (3.724)			−12.267	

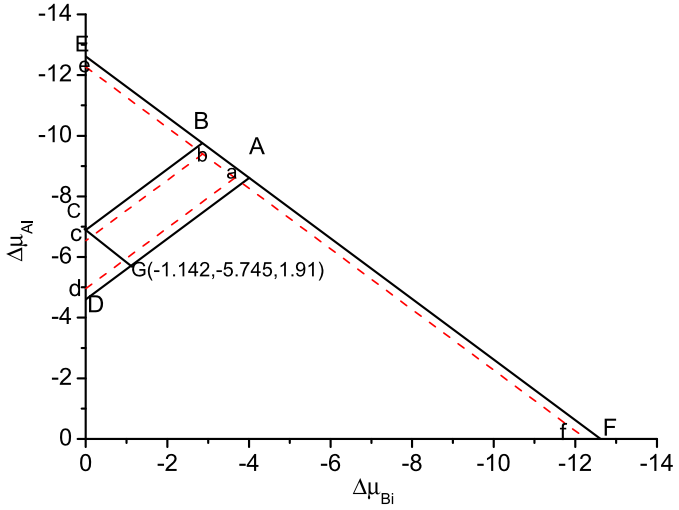

Fig. 2. The theoretical allowed chemical potential regions for $BiAlO_3$ with space group *R3c* and *Pm3m* are restricted within A-B-D-C and a-b-c-d regions, respectively. The line EF or ef denotes $\Delta\mu_O = 0$ in *R3c* and *Pm3m* systems. The Bi_2O_3 phase limits the stable chemical potential region for $BiAlO_3$ above the line CB or cb, while the limitation by the Al_2O_3 phase prohibit the chemical potential region for $BiAlO_3$ above the line DA or da.

aluminum and oxygen are constrained in a small region within A-B-D-C for *R3c* structure and a-b-c-d for *Pm3m* structure as shown in Fig. 2. It can be seen that the allowed chemical potential range for *Pm3m* structure is narrower than that of *R3c* structure. Practically the chemical potential of oxygen is often used for controlling the sintering of a compound in experiments, and then the tunable range of chemical potential for oxygen is very important to the formation of vacancy in $BiAlO_3$. Fig. 2 shows that, the oxygen chemical potential can be varied within $-2.67\ \text{eV} \leqslant \Delta\mu_O \leqslant 0$ for $BiAlO_3$ sample of *R3c* structure and $-2.42\ \text{eV} \leqslant \Delta\mu_O \leqslant 0$ for that of *Pm3m* structure. When $\Delta\mu_O$ is fixed (a serial of lines parallel to line EF) the range of $\Delta\mu_{Bi}$ and $\Delta\mu_{Al}$ can be varied within the same width, which is broader than that of $\Delta\mu_{Pb/Ba}$ or $\Delta\mu_{Ti}$ in $PbTiO_3$ and $BaTiO_3$ [22] samples under corresponding oxygen environment. Thus the formation energy of Bi or Al vacancies may be tuned in a larger range than that of Pb (Ba) or Ti in $PbTiO_3$ ($BaTiO_3$).

3.2. Charged vacancies in $BiAlO_3$ of space group R3c

In the $(\Delta\mu_{Bi}, \Delta\mu_{Al}, \Delta\mu_O)$ coordinate system, points A and B describe oxygen-rich sintering conditions and have the highest possible oxygen chemical potentials. Note that the point B also corresponds to Al-poor and point A to Bi-poor conditions. Oxygen-poor and Al-rich growth occurs at point D. Point C and D correspond to Bi-rich condition. For $BiAlO_3$ with space group *Pm3m*, the a-b-d-c region surrounded by the red lines has the corresponding sintering conditions.

Based on the calculated chemical potentials, the formation energies of possible charged oxygen and metal vacancies for four sintering conditions are obtained using Eq. (4), shown in Fig. 3. The image charge correction (typically within 200 meV) is not employed here, which is not expected to affect our conclusion since we are not dealing with the shallow levels of semiconductors. It is clear that the oxygen vacancy prefers +2 charge states and the metal vacancy favors −3 charge states. One can also see that the metal vacancy is easily formed not only under oxygen-rich and metal-poor sintering condition [cf. Fig. 3(a) and (b)], but also under oxygen-shortage and metal-rich [cf. Fig. 3(c)]. The formation of Al vacancy is easier than Bi vacancy under certain oxygen environment, for example at point C. This is in line with the experimental observations that the vacancies of B-site is dominating and plays an important role in improving the properties of material by B-site doping in an ABO_3 compounds [23,24]. Oxygen vacancies are the major defects under oxygen-poor and metal-rich environment (cf. Fig. 3(d)). In addition to the oxygen-poor condition, oxygen vacancies may be created at other appropriate sintering environment. For example, the formation energy of oxygen vacancy becomes lower than that of Al vacancy as the sintering condition shifts from point C to point G when the Fermi level is lower than 0.14 eV (cf. Fig. 3(c)). Namely, as the chemical potentials shift from point C to G, the oxygen vacancy becomes dominate when the Fermi level is near the VBM since the concentration of metal vacancy decreases. However, the Al-vacancy keeps dominate when the Fermi level is above 0.14 eV to VBM. As a result, the relative concentration of oxygen and aluminum vacancies can be tuned by changing the sintering environment.

It is known that the formation of oxygen vacancy is often coupled with vacancy Pb in $PbTiO_3$: Zr (PZT) [25,26]. The lead-oxygen vacancy pair is a natural intrinsic defect in PZT, which plays a crucial role in ferroelectric crystals. Moreover, Keeble et al have shown that the concentration of neutral or negative vacancy type defects increases with increasing oxygen vacancy concentration and confirmed that the vacancy defect is a $V_{Pb} - V_O$ complex using accurate positron annihilation experiments [27]. Therefore, it is interesting to study the Bi–O divacancy in $BiAlO_3$ materials in analogy to Pb–O divacancy in PZT. Fig. 4 shows the dependence of the formation energy ΔH of charged Bi–O bivacancy on Fermi level under bismuth-rich and oxygen-poor environment (point C) as well as bismuth-poor and oxygen-rich environment (point A). It can be seen that, the −1 charge state is preferred for the $V_{Bi} - V_O$ divacancy when E_F is located near the VBM, and as the Fermi level moving toward the CBM the favorable charge state of the divacancy becomes −2. The formation energy of the charged bivacancy is lower under Bi-poor and oxygen-rich sintering condition (point A). The formation of the charged Bi–O bivacancy gets more difficult when the environment shifts towards point G. In comparison with the formation energy of oxygen vacancy under the same condition, the energy needed to form charged Bi–O divacancy is very high, indicating the formation of Bi–O divacancy is very hard.

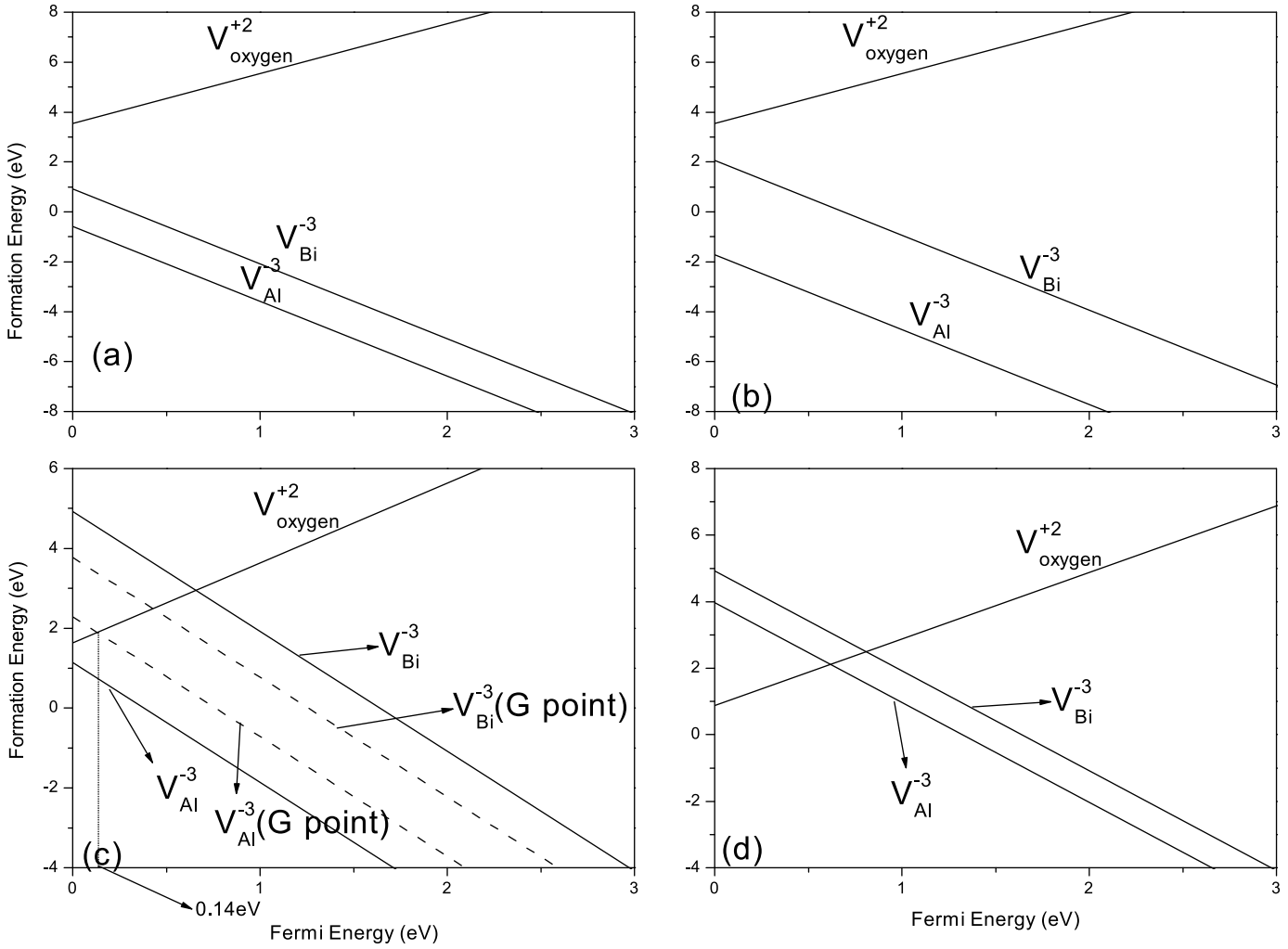

Fig. 3. The formation energy of charged vacancies under different sintering conditions. (a) For point A with $\Delta\mu_A = (-4.007, -8.61, 0)$; (b) for point B with $\Delta\mu_B = (-2.754, -9.752, 0)$; (c) for point C with $\Delta\mu_C = (0, -6.887, -1.91)$; (d) for point D with $\Delta\mu_D = (0, -4.607, -2.67)$. Only the formation energy of the stable charged state is shown.

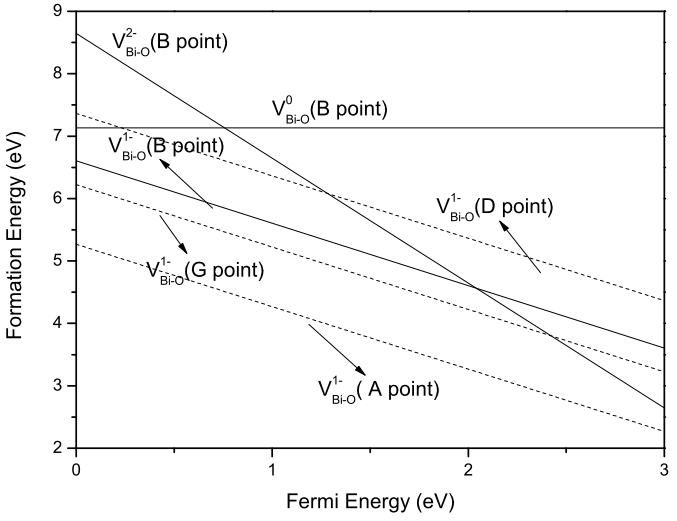

Fig. 4. The formation energy of bismuth–oxygen vacancy pairs vs Fermi level for $BiAlO_3$ under Bi-rich and O-poor (point C) and B-poor and O-rich (point D) conditions, as well as point A and point G that holds the same oxygen environment with point C.

3.3. *Vacancies in $BiAlO_3$ of Pm3m symmetry*

For $BiAlO_3$ with space group *Pm3m*, the types of possible charged vacancies are similar to those in $BiAlO_3$ with space group *R3c*. Therefore, we merely focus our attention on the neutral vacancy for the comparison of the vacancy formation in two structures. The calculated formation energy is given in Table 3 for Bi, Al, O single vacancy and Bi–O divacancy. Our calculated results show that the order of ΔH for several vacancies is the same for the two different structures. The order of oxygen vacancy is all the same 3–6 eV, and the energy needed for creating B-site vacancy is lower in $BiAlO_3$ with *R3c* structure. ΔH for A-site vacancy is a little higher than that of $PbTiO_3$ with its order about 5 eV. From Table 3, one also sees that under the condition of species j being rich $\mu_j = 0$, all vacancies in *R3c* structure have a higher formation energy than in *Pm3m* structure.

Since in experiments the chemical potential of oxygen is often used for controlling the sintering of compounds, it is convenient to discuss the vacancy formation in the range of oxygen chemical potentials, which is constrained with $-2.67 \leqslant \Delta\mu_O \leqslant 0$ for the *R3c* structure and $-2.42 \leqslant \Delta\mu_O \leqslant 0$ for the *Pm3m* structure of $BiAlO_3$. Under oxygen-rich, the formation of oxygen vacancy requires rather high energy and is unlikely to form for both struc-

Table 3
Calculated vacancy formation energies for $BiAlO_3$ with space group *Pm3m* and *R3c*. the vacancy formation energy under three different conditions are given. ΔH is the formation energy needed for vacancy created under the condition $\Delta\mu = 0$, while ΔH (O-rich) and ΔH (O-poor) correspond to the vacancy formation energies under O-rich and O-poor condition, respectively. When the formation energy is within a range rather than assuming a definite value, the range is given in brackets with two boundary values.

Vacancy	*R3c*			*Pm3m*		
	ΔH (eV)	ΔH (O-rich)	ΔH (O-poor)	ΔH (eV)	ΔH (O-rich)	ΔH (O-poor)
V_{Bi}	4.919	[0.912, 2.065]	4.919	6.563	[2.943, 3.693]	6.563
V_{Al}	8.033	[−1.749, 0.577]	3.426	11.203	[1.863, 2.573]	6.273
V_{Bi-O}	9.802 (point E)	[7.048, 5.795]	7.132	7.05 (point E)	[3.43, 4.18]	4.612
V_O	3.539	3.539	0.869	6.39	6.39	3.97

tures. Therefore, we need only compare the metal-vacancy and Bi–O divacancy for the structures. Under oxygen-rich condition, the formation energy of metal vacancies is lower than that of oxygen vacancy, and that of Bi–O bivacancy is highest. The formation energy of Al vacancy falls into the range of −2 eV–0.6 eV, and then it is quite easy to form and dominates the defect in the *R3c* structure. Although the formation energy of Al vacancy is the lowest in all the possible vacancies in the *Pm3m* structure, it is still very difficulty to form due to its high formation energy. In addition, the range of formation energy of metal vacancy in the *Pm3m* structure is about 0.7 eV, lower than that in *R3c* structure (2.2 eV). It demonstrates that the adjustable range of chemical potential of oxygen is smaller for *Pm3m* structure. Under oxygen-poor, oxygen vacancy will be the dominating defect. Similarly, the formation energy of oxygen vacancy is found to be lower in *R3c* structure. Therefore, it is clear that the concentration of oxygen vacancy in *R3c* structure is relatively higher than that in *Pm3m* structure. In a word, the formation of vacancy for compound in the *Pm3m* structure is more difficult than that of compound in the *R3c* structure under the corresponding condition.

4. Conclusions

Formation energies of different charged vacancies in $BiAlO_3$ with *R3c* and *Pm3m* symmetries are studied by first-principles calculation. We find that the adjustable range of valid chemical potential for *Pm3m* symmetry material is narrower than that of *R3c* structure. Possible charged vacancies in compounds have mostly oxygen vacancy with +2 charge state, Bi- and Al-vacancy with −3 charge state as well as Bi–O divacancy with −1 charge state. It shows that the charged metal vacancy is prevalent under metal-poor and oxygen-rich. The charged oxygen vacancy can easily be found under oxygen-poor environment. The formation energy of Bi–O divacancy is very high and can be difficultly obtained. According as the formation energy and chemical potentials, formation energies of neutral vacancies under different sintering conditions are studied for two different symmetry $BiAlO_3$. Results reveal that possible vacancies are more easily formed in *R3c* system than in *Pm3m* system under same condition.

Acknowledgements

This work was funded by NSFC Grant (Nos. 50772039 and 10704025) through NSFC Committee of China and the Foundation (No. 07118058) through the Science and Technology Bureau of Guangdong Government respectively.

References

[1] S.Y. Yang, F. Zavaliche, L. Mohaddes-Ardabili, V. Vaithyanthan, D.G. Schlom, Y.J. Lee, Y.H. Chu, M.P. Cruz, Q. Zhan, T. Zhao, R. Ramesh, Appl. Phys. Lett. 87 (2005) 102903.
[2] A.A. Belik, T. Wuernisha, T. Kamiyama, K. Mori, M. Maie, T. Nagai, Y. Matsui, E. Takayama-Muromachi, Chem. Mater. 18 (2006) 133.
[3] R.E. Cohen, Nature. 358 (1992) 136.
[4] N.A. Hill, K.M. Rabe, Phys. Rev. B 59 (1999) 8759.
[5] P. Baettig, C.F. Schelle, R. LeSar, U.V. Waghmare, N.A. Spaldin, Chem. Mater. 17 (2005) 1376.
[6] J. Zylberberg, A.A. Belik, E. Takayama-Muromachi, Z.G. Ye, Chem. Mater. 19 (2007) 6385.
[7] C. Elissalde, J. Ravez, J. Mater. Chem. 11 (2001) 1957.
[8] E. Cockayne, B.P. Burton, Phys. Rev. B 69 (2004) 144116.
[9] J.M.D. Coey, M. Venkatesan, C.B. Fitzgerald, Nat. Mater 4 (2005) 173.
[10] H. Meštrić, R.A. Eichel, T. Kloss, K.P. Dinse, So. Laubach, St. Laubach, P.C. Schmidt, K.A. Schönau, M. Knapp, H. Ehrenberg, Phys. Rev. B 71 (2005) 134109.
[11] Lixin He, David Vanderbilt, Phys. Rev. B 68 (2003) 134103.
[12] O.N. Tufte, P.W. Chapman, Phys. Rev. 155 (1967) 796.
[13] S.B. Zhang, J.E. Northrup, Phys. Rev. Lett. 67 (1991) 2339.
[14] Yu-Jun Zhao, Alex Zunger, Phys. Rev. B 69 (2004) 175208.
[15] G. Kresse, J. Hafner, Phys. Rev. B 47 (1993) 558;
G. Kresse, J. Hafner, Phys. Rev. B 49 (1994) 14251.
[16] M.R. Pederson, K.A. Jackson, Phys. Rev. B 43 (1991) 7312.
[17] P.E. Blöchl, Phys. Rev. B 50 (1994) 17953.
[18] Chenliang Li, Biao Wang, Rui Wang, Hai Wang, Xiaoyan Lu, Physica B 403 (2008) 539.
[19] Hai Wang, Biao Wang, Rui Wang, QingKung Li, Physica B 390 (2007) 96.
[20] Zhaojun Liu, Xuejie Huang, Dingsheng Wang, Solid State Communication 147 (2008) 505.
[21] CRC Handbook of Chemistry and Physics, Taylor and Francis, Boca Raton, FL, 2007.
[22] Z. Alahmed, H.X. Fu, Phys. Rev. B 76 (2007) 224101.
[23] B. Noheda, J.A. Gonzalo, L.E. Gross, R. Guo, S.E. Park, D.E. Cox, G. Shirane, Phys. Rev. B 61 (2000) 8687.
[24] M. Brazier, S. Mansour, M. McElfresh, Appl. Phys. Lett. 74 (1999) 4032.
[25] J.F. Scott, C.A. Araujo, B.M. Melnick, L.D. McMillan, R. Zuleeg, J. Appl. Phys. 70 (1991) 382.
[26] H. Maiwa, N. Ichinose, K. Okazaki, J. Jpn. Appl. Phys. Part 1 33 (1994) 5240.
[27] D.J. Keeble, B. Nielsen, A. Krishnan, K.G. Lynn, S. Madhukar, R. Ramesh, C.F. Young, Appl. Phys. Lett. 73 (1998) 7789.